Available online at www.sciencedirect.com
ScienceDirect
Journal of the European Ceramic Society 30 (2010) 1519–1526
www.elsevier.com/locate/jeurceramsoc

The carbon nonstoichiometry and the lattice parameter of $(Ti_{1-x}W_x)C_{1-y}$

S. Park [a], J. Jung [a], S. Kang [a,*], B.W. Jeong [b], C.-K. Lee [b], J. Ihm [b]

[a] *Department of Materials Science and Engineering, Seoul National University, Seoul 151-742, Republic of Korea*
[b] *Department of Physics and Center for Theoretical Physics, Seoul National University, Seoul 151-742, Republic of Korea*

Received 24 June 2009; received in revised form 18 October 2009; accepted 28 October 2009
Available online 27 November 2009

Abstract

Various monolithic (Ti,W)C powders were synthesized from mixtures of carbon and oxides by varying the W content. The carbon content in the (Ti,W)C solid solution decreased with increasing W content when the solid solution was sintered at 1510 °C for 1 h. The lattice parameters of the sintered (Ti,W)C ceramics tend to decrease with carbon content. In this study, the changes in the carbon content as a function of the tungsten content were compared with the results obtained using ThemoCalc® software. The relationship between the lattice parameter and composition was examined using an analytical approach and *ab initio* simulations.

Keywords: (Ti,W)C; Lattice parameter; Carbon content; *Ab initio*; ThermoCalc®

1. Introduction

Monolithic (Ti,W)C is a solid solution of TiC and WC that has been in demand by the hard materials industry since the 1980s.[1,2] Recent advances in processing carbides have rendered an economical way of producing such materials, including more complex materials, such as (Ti,W,M1,M2)C- or (Ti,W,M1,M2)(CN)-type solid solutions.[3–6] These materials have the same *B*1(*NaCl*) crystal structure as TiC, as well as other excellent properties of TiC, such as high hardness, chemical stability, and deformation resistance at high temperatures. Especially, these solid solutions offer significantly improved toughness,[6] which has been in demand to overcome the application limits of TiC- and Ti(CN)-based cermets and ceramics.

Generally, TiC is a nonstoichiometric compound, and fully annealed TiC shows a Ti:C mole ratio of 1:0.98. The carbon deficiency in the compound varies with temperature and the addition of other elements in the form of a solid solution. Therefore, a change in the stoichiometry of $(Ti,W)C_{1-y}$ as a function of a secondary element, W in this case, is an interesting and important issue in the development of such solid solution carbides.[7]

W and C form stoichiometric WC with a *hcp* structure at low temperatures. By contrast, WC, with a *B*1(*NaCl*) structure, is only stable above 2500 °C.[8] Two separate phases, (Ti,W)C and WC, are formed when excessive amounts of WC are added to TiC, due to their limited solubilities. The solubility limit, *x*, of W in the $(Ti_{1-x}W_x)C$ phase is reported to be ~0.5.[6] When it exceeds this limit, pure WC co-exists with (Ti,W)C in the microstructures.

In this study, a monolithic (Ti,W)C solid solution powder was synthesized by milling mixtures of oxides and carbon powder. The change in the carbon content was investigated as a function of the W content in the solid solution, and the results were compared with those obtained using ThermoCalc® software. An analytical investigation was undertaken to help understand the behavior of C and W in the solid solution phases by measuring the lattice parameters. Furthermore, the results of *ab initio* simulations via pseudo-potential total energy calculations were used for comparison.

2. Experimental procedure

The (Ti,W)C powders were produced using anatase TiO_2 (99+ % purity, <40 μm, Sigma–Aldrich), WO_3 (99+ % purity, <20 μm, Sigma–Aldrich), and C (99.9%, 10 μm, Curcuma Longa). Assuming that the carbon in the system reduces all of the oxides to carbon monoxide (CO), the raw materials were weighed carefully to produce stoichiometric $(Ti_{1-x}W_x)C$. The target value of *x* was varied from 0.05 to 0.5, i.e., 5–50 at.%. The

* Corresponding author. Tel.: +82 2 880 7167; fax: +82 2 884 1413.
E-mail address: shinkang@snu.ac.kr (S. Kang).

0955-2219/$ – see front matter © 2009 Elsevier Ltd. All rights reserved.
doi:10.1016/j.jeurceramsoc.2009.10.022

oxide mixtures were subjected to high-energy ball milling using a planetary mill (Fritsch Pulverisette 5). The WC–Co balls (as the milling medium) were mixed with the oxide mixtures and carbon at a ball-to-powder weight ratio of 40:1. All milling procedures were carried out at a speed of 250 rpm for a period of 20 h in tungsten carbide bowls that were initially purged and filled with Ar. The final (Ti,W)C powders were prepared by carbothermal reduction under vacuum ($\sim 10^{-4}$ atm), at 1200 or 1300 °C, for 1 h.

The powders were reduced carbothermally and subsequently analyzed with a Carbon analyzer (Leco WC-200AC USA), Nitrogen/Oxygen analyzer (Leco TC-436 USA), and X-ray diffraction (XRD, M18XHF-SRA, Macscience, Japan) with Si as the reference. The powders were compacted into disks, each 1 cm in diameter, under a pressure of 125 MPa. They were then sintered at 1510 °C for 1 h under vacuum ($\sim 10^{-4}$ atm). The lattice parameters of the powders and sintered samples were calculated using the Nelson–Riley method.[9] The grain sizes of the carbides were calculated using Scherrer's formula.[10] The ternary phase diagram for Ti–W–C was obtained using the ThermoCalc® program.

Ab initio pseudo-potential total energy calculations were performed using the plane-wave basis set. This was done in order to understand the structure and energetics of the $(Ti_{1-x}W_x)C$ system in more detail.[11] The Generalized Gradient Approximation to the Density Functional Theory and Vanderbilt ultrasoft pseudo-potentials, generated with a Scalar-Relativistic Calculation for W and Ti and non-relativistically for C was used.[12,13] The $(Ti_{1-x}W_x)C$ system was simulated using the supercell method with 64 atoms per unit cell. For the total energy calculation, the Brillouin zone was sampled according to the Monkhorst-Pack scheme, and the irreducible *k*-point numbers were varied from 6 to 8, depending on the unit cell. The cutoff energy for the plane-wave basis was 55 Ry. The atomic positions were fully relaxed until all of the force components were smaller than 10^{-3} Ry/a_B.

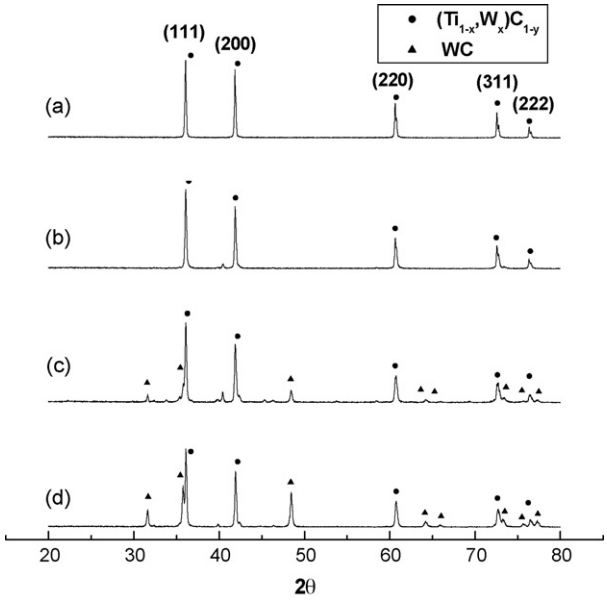

Fig. 1. XRD analysis of powders synthesized at 1300 °C for 1 h by the carbothermal reduction: (a) $(Ti_{0.8}W_{0.2})C$, (b) $(Ti_{0.7}W_{0.3})C$, (c) $(Ti_{0.6}W_{0.4})C$ and (d) $(Ti_{0.5}W_{0.5})C$.

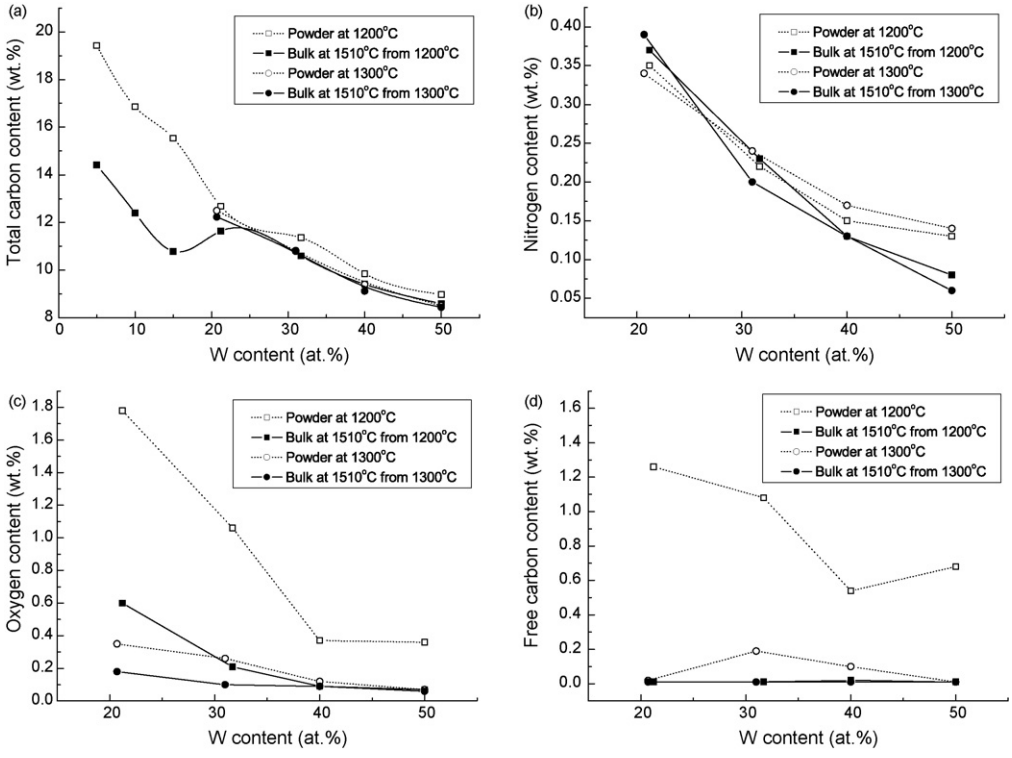

Fig. 2. The CNO analysis of various $(Ti_{1-x}W_x)C_{1-y}$ powders: (a) total carbon, (b) nitrogen, (c) oxygen and (d) free carbon.

3. Results and discussion

3.1. (Ti,W)C solid solution powder

Fig. 1 shows the XRD results of the powders synthesized after carbothermal reduction at 1300 °C for 1 h. The peaks for (Ti,W)C and WC were identified in the systems. Complete solid solutions were synthesized in the $(Ti_{0.8}W_{0.2})C$ and $(Ti_{0.7}W_{0.3})C$ systems, whereas the target compositions of $(Ti_{0.6}W_{0.4})C$ and $(Ti_{0.5}W_{0.5})C$ contained (Ti,W)C and WC phases. A similar result was obtained for the powders synthesized at 1200 °C for 1 h with the higher amounts of WC, i.e. $(Ti_{0.6}W_{0.4})C$ and $(Ti_{0.5}W_{0.5})$. These results suggest that increasing the processing temperature increases the solubility limit for W in (Ti,W)C.

Fig. 2 shows the results of the CNO(carbon/nitrogen/oxygen) analysis for the powders synthesized at 1200 and 1300 °C. In both powders, the amounts of nitrogen and oxygen decrease with increasing W in (Ti,W)C (Fig. 2b and c). The oxygen content is more affected by the reduction temperature than the nitrogen content is. It is because the carbothermal reduction is controlled by the processing temperature and the degree of noncrystallinity in the milled oxide mixture. The powder synthesized at 1300 °C has lower oxygen content than that produced at 1200 °C. The oxygen content was much lower after sintering in both cases than before sintering.

In terms of the total carbon content, there was no significant difference between the powder and sintered ceramics (Fig. 2a). This was particularly true for the powder synthesized at 1300 °C. This means that the stable (Ti,W)C compositions are already obtained during powder synthesis, when x in $(Ti_{1-x}W_x)C$ exceeds 0.2. However, the carbon content of the powder synthesized at 1200 °C shows a significant difference of ~5 wt.% for low W compositions ($x < 0.15$). The amount of free carbon in the powders was also somewhat high for the powder synthesized at 1200 °C, even if the amount was negligible (<0.2 wt.%) after sintering. This is consistent with the trend of total carbon. The decreases in the total and free carbon contents were attributed to the loss of carbon during the high temperature processing and the formation of an equilibrium (Ti,W)C phase.

3.2. Stoichiometry and lattice parameters of (Ti,W)C ceramics

Ceramic bulk samples were prepared at 1510 °C for 1 h using the powders that had been synthesized at 1200 or 1300 °C for 1 h. Fig. 3 shows the XRD patterns of the samples made from the powders produced at 1300 °C. There was no change in the phases formed at the two synthesis temperatures after the sintering process, except for the WC content in the $(Ti_{0.6}W_{0.4})C$ and $(Ti_{0.5}W_{0.5})C$ systems. The $(Ti_{0.6},W_{0.4})C$ system, which is made from the powder synthesized at 1300 °C, no longer has a WC phase after sintering at 1510 °C. This is thought to be due to the increased solubility limit of WC. However, both the sintered $(Ti_{0.6}W_{0.4})C$ and $(Ti_{0.5}W_{0.5})C$ ceramics made from the powders synthesized at 1200 °C contained (Ti,W)C and WC.

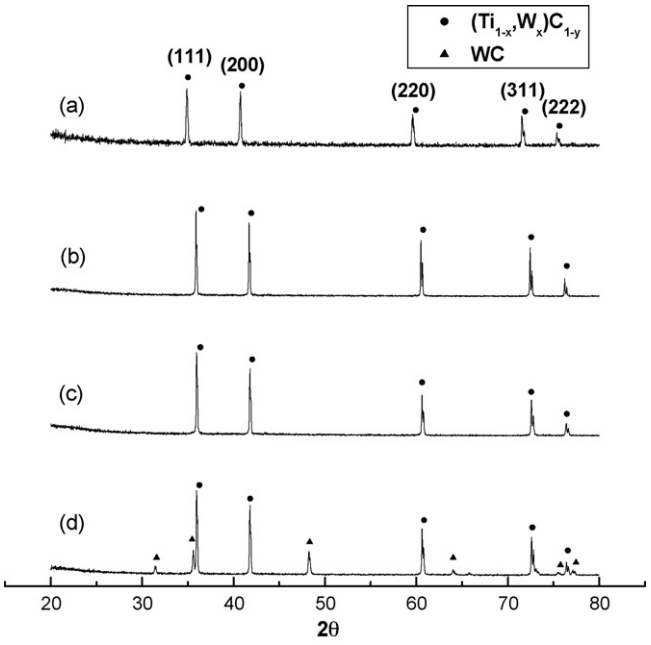

Fig. 3. XRD analysis of ceramics sintered at 1510 °C. The following powders were synthesized at 1300 °C for 1 h: (a) $(Ti_{0.8}W_{0.2})C$, (b) $(Ti_{0.7}W_{0.3})C$, (c) $(Ti_{0.6}W_{0.4})C$, and (d) $(Ti_{0.5}W_{0.5})C$.

Table 1 shows the compositions calculated from the results of TEM/EDS and CNO analyses (Fig. 2). In all compositions, the W concentrations were relatively uniform, irrespective of the locations observed in the grains. The measured W content was more than what was added to the system. The W contents were slightly higher than the intended values in all systems except for some compositions, such as $(Ti_{0.6}W_{0.4})C$ (made at 1200 °C) and $(Ti_{0.5}W_{0.5})C$ (made at 1200 and 1300 °C). This was attributed to W contamination from the WC–Co milling balls.

Table 1
The carbon content in the (Ti,W)C ceramics along with the values calculated by ThermoCalc® at 1510 °C.

Target compositions	Ceramics sintered at 1510 °C from 1200 °C	Ceramics sintered at 1510 °C from 1300 °C	ThermoCalc® at 1510 °C
$(Ti_{0.95}W_{0.05})C$	$(Ti_{0.95}W_{0.05})C_{0.784}$[a]		
$(Ti_{0.90}W_{0.10})C$	$(Ti_{0.90}W_{0.10})C_{0.743}$[a]		
$(Ti_{0.85}W_{0.15})C$	$(Ti_{0.85}W_{0.15})C_{0.702}$[a]		
$(Ti_{0.80}W_{0.20})C$	$(Ti_{0.788}W_{0.212})C_{0.850}$	$(Ti_{0.793}W_{0.207})C_{0.887}$	$(Ti_{0.8}W_{0.2})C_{0.855}$–$(Ti_{0.8}W_{0.2})C_{0.938}$
$(Ti_{0.70}W_{0.30})C$	$(Ti_{0.683}W_{0.317})C_{0.902}$	$(Ti_{0..690}W_{0.310})C_{0.911}$	$(Ti_{0.7}W_{0.3})C_{0.852}$–$(Ti_{0.7}W_{0.3})C_{0.931}$
$(Ti_{0.60}W_{0.40})C$	$(Ti_{0.598}W_{0.402})C_{0.887}$	$(Ti_{0.580}W_{0.420})C_{0.879}$	$(Ti_{0.6}W_{0.4})C_{0.838}$–$(Ti_{0.6}W_{0.4})C_{0.898}$
$(Ti_{0.50}W_{0.50})C$	$(Ti_{0.568}W_{0.432})C_{0.896}$	$(Ti_{0.524}W_{0.476})C_{0.885}$	$(Ti_{0.5}W_{0.5})C_{0.838}$–$(Ti_{0.5}W_{0.5})C_{0.852}$

[a] The W content was not analyzed. It is expected to be slightly higher than the target values.

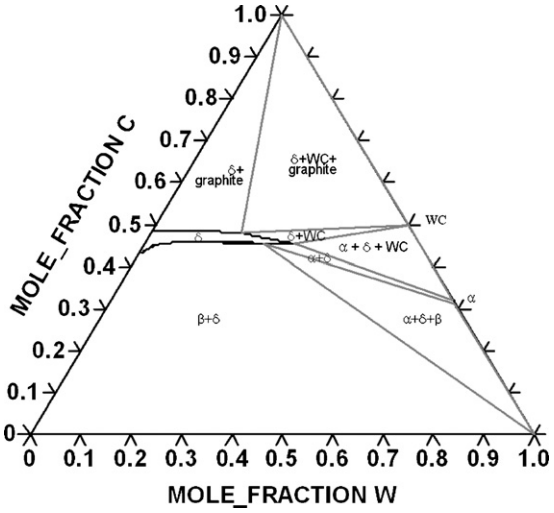

Fig. 4. Calculated phase diagram of Ti–W–C at 1510 °C using ThermoCalc®: $\delta(Ti_{1-x},W_x)C_{1-y}$.

Using ThermoCalc® software, the ternary phase diagram of Ti–W–C at 1510 °C was calculated to confirm the stable phase field boundary and compositions, as shown in Fig. 4. A NaCl crystal structure, (Ti,W)(C,V), where V stands for a vacancy, was used for the calculation. The phase region where the (Ti,W)C solid solution phase exists is widespread with respect to the W content. However, it becomes narrow with respect to the carbon content. According to the calculations, W can replace up to 55.2 at.% of the Ti in the TiC sublattice at 1510 °C. The calculated composition is $(Ti_{0.447}W_{0.552})C_{0.844}$.

Table 1 also reports the calculated carbon range for a fcc solid solution at the specific Ti to W ratios. In general, the carbon content decreases with increasing W content in (Ti,W)C. The samples prepared for the $(Ti_{0.8}W_{0.2})C$, $(Ti_{0.7}W_{0.3})C$, and $(Ti_{0.6}W_{0.4})C$ target compositions have carbon contents that are within the carbon content ranges predicted by ThermoCalc®. This is not the case for samples made to have the target composition $(Ti_{0.5}W_{0.5})C$. This is because excess W in the (Ti,W)C separates from the solid solution, in the form of WC, at the sintering temperature. Nevertheless, this somewhat contradicts the result from the phase diagram.

It should be noted that the final compositions, $(Ti_{0.568}W_{0.432})C_{0.896}$ at 1200 °C or $(Ti_{0.524}W_{0.476})C_{0.885}$ at 1300 °C, which are in equilibrium with WC, are somewhat different from the predicted composition, $(Ti_{0.447}W_{0.552})C_{0.844}$. In addition, the measured carbon content in the sintered ceramics is almost independent of W. This indicates that the carbon in the $(Ti_{1-x}W_x)C$ phase has a higher stability in the vicinity of 1510 °C than predicted. TiC and WC powders are often synthesized at temperatures higher than 1700, 1300 °C, respectively.[14] The input data of ThermoCalc® is based on these results. Thus, the relatively low processing temperature of 1200–1300 °C used in this study might be the cause of the difference.

The lattice parameters of (Ti,W)C with various compositions were obtained using the Nelson–Riley method. Fig. 5 shows the results of the various $(Ti_{1-x}W_x)C_{1-y}$ ceramics synthesized (Curve E). The lattice parameter of the complete solid solution tends to increase with increasing carbothermal reduction temperature. The behavior of the lattice parameter is affected by the extent of powder carburization. As the mole fraction of W exceeds 0.2, the change in the lattice constant becomes insensitive to that of the W content, particularly for the samples made from the powders synthesized at 1200 °C. This was attributed to the adjustment in the solubility of W atoms and the carbon content in the system. Generally, the addition of W is reported to reduce the lattice parameter in the region of (Ti,W)C formation.[14] Both the small size of the W atom in the TiC structure and the loss of carbon cause the decrease in the lattice parameter. The lattice parameter of annealed TiC is 4.3274 Å.[15]

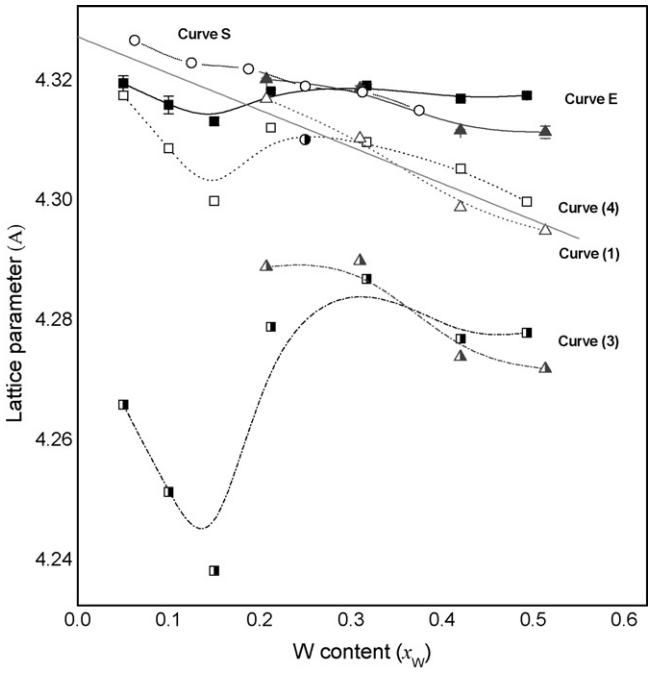

Fig. 5. The change in the lattice parameter of nonstoichiometric $(Ti_{1-x}W_x)C_{1-y}$ as a function of W content: Curve E : experimental bulk from 1200 to 1510 °C (■), 1300 to 1510 °C (▲), Curve (1): a straight line obtained using Eq. (1) based on the stoichiometric $(Ti_{1-x}W_x)C_{0.98}$, Curve (3): 1200–1510 °C bulk calculated by Eq. (3) (◨), 1300–1510 °C bulk calculated by Eq. (3) (◭), Curve (4): 1200–1510 °C bulk calculated by Eq. (4) (□), 1300–1510 °C bulk calculated by Eq. (4) (△).

The lattice parameters measured for the sintered (Ti,W)C samples (having various W contents) were quite different from those based on the general expectation that the lattice parameters of the solid solutions decrease almost linearly. The ceramics of (Ti,W)C made from the powders synthesized at 1200 °C with a low W content ($x < 0.2$) have smaller lattice parameters with a significant initial drop than the expected values. It requires further investigation to explain this behavior. For the ceramics obtained from the powders synthesized at 1300 °C with W contents of >0.2, the lattice parameters tend to decrease with increasing W content.

3.3. Lattice parameters by an analytical approach

A simple model was used to explain the behavior of the lattice parameters of $(Ti_{1-x}W_x)C_{1-y}$, assuming that the change in

the lattice parameters follows Vegard's law, and that all solid solutions are in the form of $(Ti_{1-x}W_x)C_{0.98}$ without a loss of carbon. In addition, every carbide and metallic phase contained in the carbide were assumed to have *B*1(*NaCl*) and fcc structures, respectively. The measured lattice parameter of $TiC_{0.98}$, $a[TiC_{0.98}(B1)]$ was 4.3274 Å.[15] The values of a[WC(*B*1)], a[Ti(fcc)], and a[W(fcc)], calculated by *ab initio* method were 4.2662, 4.06, and 4.00 Å, respectively.[16,17]

For $(Ti_{1-x}W_x)C_{0.98}$, the lattice parameter can be expressed as follows:

$$a[(Ti_{1-x}W_x)C_{0.98}] = (1-x)\cdot a[TiC_{0.98}(B1)] + x\cdot a[WC(B1)] \quad (1)$$

Similarly, based on the above assumptions, the lattice parameter of the $(Ti_{1-x}W_x)$ (fcc) solid solution with no carbon was determined as follows:

$$a[Ti_{1-x}W_x(fcc)] = (1-x)\cdot a[Ti(fcc)] + x\cdot a[W(fcc)] \quad (2)$$

Therefore, a general equation for $a[(Ti_{1-x}W_x)C_{1-y}]$ can be obtained by Vegard's law, as shown below for y ranging from 0.02 to 1.

$$a[(Ti_{1-x}W_x)C_{1-y}] = a[(Ti_{1-x}W_x)C_{0.98}] - \frac{a[(Ti_{1-x}W_x)C_{0.98}] - a[Ti_{1-x}W_x(fcc)]}{0.98}\cdot(y-0.02) \quad (3)$$

Eq. (1) was established for $(Ti_{1-x}W_x)C_{0.98}$, assuming that the carbon content was fixed at 0.98, while Eq. (3) allows carbon loss in $(Ti,W)C_{1-y}$, which is more realistic. Curves (1) and (3), determined using Eqs. (1) and (3), respectively, are drawn in Fig. 5 along with the measured data in Table 1 (Curve E). However, Curve (1) shows a better fit to the experimental values (Curve E) than Curve (3) does. On the other hand, Curve (3) resembles Curve E in shape, even though there is a difference in magnitude. This suggests that the simple analytical expression based on Vegard's law explains the behavior of the lattice parameter of $(Ti,W)C_{1-y}$ rather accurately. In addition, the change in the lattice parameter is almost analogous to that of the carbon content with respect to the W content, as shown in Fig. 6. The lattice parameter is affected more by the C content than by the W content.

As an alternative approach, $(Ti_{1-x}W_x)C_{1-y}$ was assumed to form from WC and TiC_{1-y} (excluding $TiC_{0.98}$), as shown in Eq. (3). This was based on the experimental results of the formation of a solid solution. In this study, $(Ti_{1-x}W_x)C_{1-y}$ was synthesized from TiO_2, WO_3, and C. The WC phase completes to form below 1000 °C and co-exists with the TiC located at a shifted diffraction angle (=2θ) above 1000 °C.[4] The peak shift is often attributed to carbon deficient TiC_{1-y} having a high oxygen content, and to the existence of W. Therefore, the solid solution is believed to form directly from $TiC_{1-y}O_y$ and WC contents during the reduction.

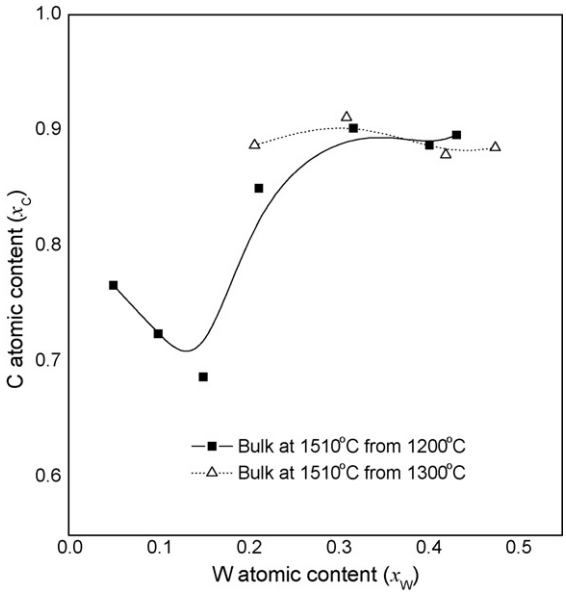

Fig. 6. The carbon content (at.%) in (Ti,W)C sintered at 1510 °C obtained by C/N/O analysis.

Furthermore, nonstoichiometric TiC_{1-y} has a wide region of homogeneity above 1200 °C from $TiC_{0.48}$ to $TiC_{0.98}$.[18] The carbon content in WC ranges from 37 to ~48 at.%. For reaction (4) below, the value, $y'(=y/(1-x))$, in $TiC_{1-y'}$ can be predicted from the measured compositions.

$$(1-x)TiC_{1-y'} + xWC = (Ti_{1-x}, W_x)C_{1-y} \quad (4)$$

A more realistic lattice parameter of TiC_{1-y} can be obtained from the empirical values. The lattice parameter of TiC_{1-y} decreases linearly with increasing carbon content after an initial short increase.[19] This means that the lattice parameter increases almost linearly from a carbon content of 0.98 to 0.86 (=1 − y), but decreases almost linearly from 0.86 to 0.47.[18,20]

Based on reaction (4), the lattice parameters of various compositions were calculated using the lattice parameters of $TiC_{1-y'}$ and WC (*B*1). The results of the calculation are shown as Curve (4) in Fig. 5. They were found to closely match with Curve (1), approaching the experimental results. This reconfirms that a $(Ti_{1-x}W_x)C_{1-y}$ solid solution is formed from nonstoichiometric $TiC_{1-y'}$ and WC. However, the mechanism for the $(Ti_{1-x}W_x)C_{1-y}$ formation requires further study.

Vegard's law does not reflect the interactions between atoms caused by alloying. That is, Eq. (3) determines the lattice parameter of a solid solution using the mean bond lengths of bonds such as Ti–C and W–C. The bond strength between W and C is weaker in the *B*1 structure than in the stable hexagonal structure, even within the range of W solubility. The change in the parameter for $(Ti,W)C_{1-y}$ would reflect the affinity between the atoms involved in the bonding compared with that from Eq. (3).

As shown in Table 1, the actual $(Ti_{1-x}W_x)C_{1-y}$ shows carbon loss with increasing W due to the thermodynamic stability. It implies the formation of vacancies in the solid solution. The loss of carbon might be more probable around W atoms than Ti. It is due to the difference in the electron population (covalency)

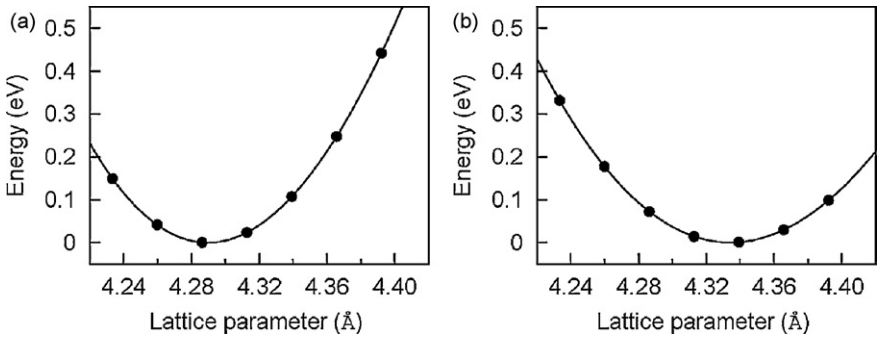

Fig. 7. Total energy per unit cell versus unit cell volume. The solid line is a fitting curve from the Birch–Murnaghan equation: (a) WC and (b) TiC.

between carbon and Ti or W in the $B1$ structure. This carbon loss causes not only the weakening of the bonds among them but also the local asymmetry.

The bonding nature of many carbides is partially metallic and covalent with little ionic character.[21] The W atoms neighboring with carbon atoms would experience weak covalent (relatively repulsive) forces compared with those neighboring vacancies. Eventually, the W atoms prefer vacancies to carbon atoms with an increase in W content in the B1 structure. This results in higher lattice parameters than those calculated by Vegard's law. This implies that the atomic interactions in $(Ti_{1-x}W_x)C_{1-y}$ play a greater role in determining the lattice parameters.

3.4. Lattice parameters by ab initio simulation

The WC phase of the $B1$ structure was observed only at high temperatures, and the lattice parameter of WC was estimated to be 4.24 Å. This is smaller than that of TiC, which is 4.327 Å.[8,22] The lattice parameters calculated in this study were 4.290 and 4.334 Å for $B1$ WC and stoichiometric $TiC_{1.0}$, respectively. These values are slightly larger than the experimental values. However, it should be noted that the experimental values were obtained from $TiC_{0.98}$ that contained some carbon vacancies. These calculated values are quite reasonable because vacancies reduce the lattice parameter. The equilibrium lattice parameters were found by fitting the total energy versus volume data using the Birch–Murnaghan equation.[23] Fig. 7 shows the total energy of TiC and WC (having NaCl structures) as a function of lattice parameter.

Fig. 5 shows that the actual lattice parameter (Curve E) decreases with increasing W concentration. In order to investigate the reduction of the lattice parameter, W atoms were placed randomly into Ti sites of TiC having 64 atoms per unit cell. Curve S in Fig. 8 presents the calculated lattice parameters for various W contents (based on stoichiometric $TiC_{1.0}$), along with the experimental data in Fig. 5. These results show that the calculated equilibrium volumes almost obey Vegard's law $[V_{eq}(x) = (1-x)V_{eq}{}^{TiC} + xV_{eq}{}^{WC(NaCl)}]$,[24] and that they match those measured experimentally (Curve E, synthesized and sintered at 1300 and 1510 °C, respectively). This means that the reduction of the lattice parameter is primarily due to the smaller atomic radius (1.35 Å) of the W atom than that (1.40 Å) of the Ti atom in the structure. Based on this Curve S, it can be said that the effect of carbon loss on the lattice parameter is nearly the same as that of atomic (electronic) interactions. That is, the effect of vacancies on the lattice parameter seems to be compensated by the presence of relatively weak bonding between W and C in the NaCl($B1$) structure.

In addition, a highly symmetric structure of $(Ti_{0.75}W_{0.25})C_{1.0}$ with a $L1_2$ structure was examined, where W atoms were in good order.[25] The $L1_2$ structure is depicted as an inset in Fig. 8. The ground state of the $L1_2$ structure provides a smaller lattice parameter (4.310 Å) than a random configuration, suggesting that the $L1_2$ structure is unlikely to form in the (Ti,W)C system. The lattice parameters were also checked in two different cases where W atoms were distributed randomly and clustered together. Fig. 9 shows these configurations for $(Ti_{0.8125}W_{0.1875})C_{1.0}$. The equilibrium lattice constants are essentially the same within computational uncertainty. Therefore, considering the entropic

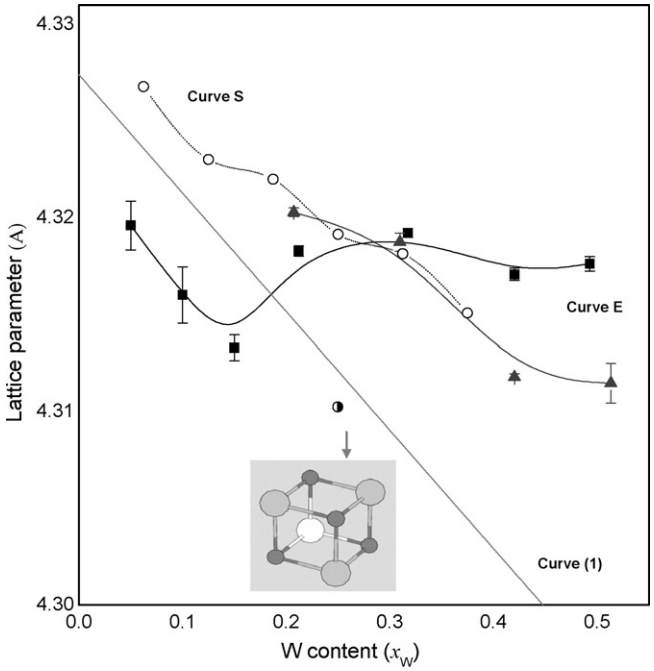

Fig. 8. The change in the lattice parameter of stoichiometric $(Ti_{1-x}W_x)C_{1.0}$, Curve S, as a function of W content, along with other data from Fig. 5: Curve S: stoichiometric $(Ti_{1-x}W_x)C$ by *ab initio* calculation (◯), $L1_2$ structure $(Ti_{0.75}W_{0.25})C_{1.0}$ (◑), Curve E: experimental bulk from 1200 to 1510 °C (■), 1300 to 1510 °C (▲).

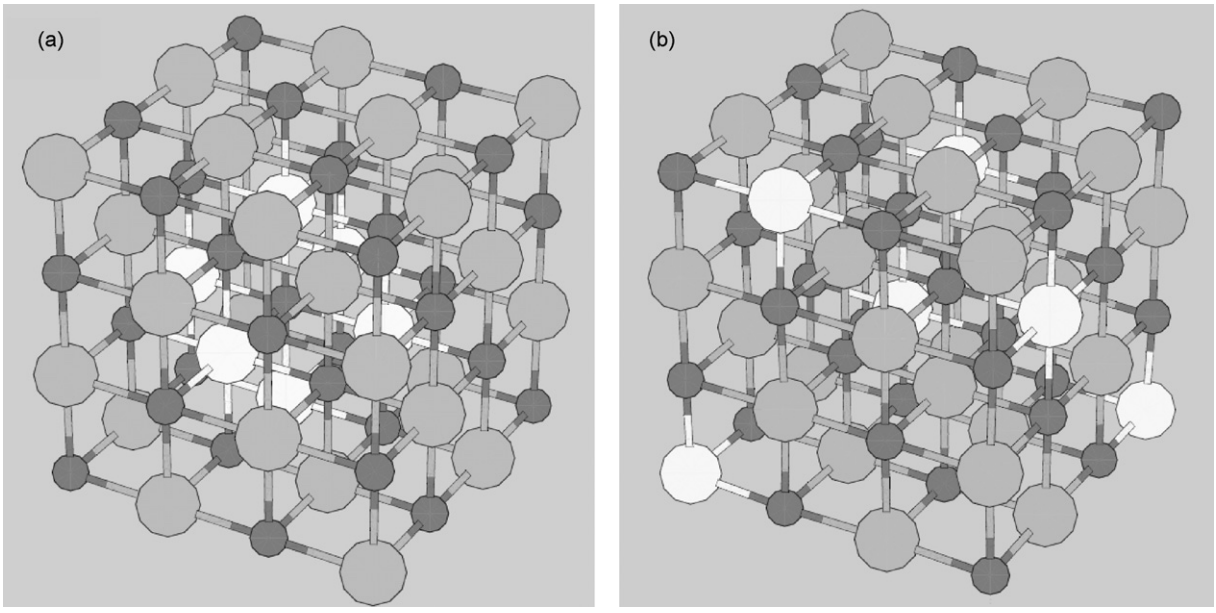

Fig. 9. Two different supercell configurations of $(Ti_{0.8125}W_{0.1875})C$: (a) supercell with clustered W atoms and (b) supercell with randomly distributed W atoms.

effect, a random distribution of W atoms is more realistic than W segregation for $(Ti_{0.8125}W_{0.1875})C_{1.0}$. This situation might change to the partial segregation of W atoms in the cell as the W content increases to the solubility limit. In addition, it is found that the bulk modulus is linearly proportional to the W content. It ranges from 250 to 290 GPa for 0–38 at.% addition of W to the TiC structure, obeying Vegard's law ($B_{av}(x) = (1-x)B^{TiC} + xB^{WC(NaCl)}$) closely.

Figs. 1 and 3 show that $(Ti_{1-x}W_x)C_{1-y}$ cannot be a single phase when x exceeds 0.4. Instead, it is a mixture of $(Ti_{1-x}W_x)C_{1-y}$ with a $B1$ structure, and WC with a *hcp* lattice. Using a similar approach to that in Fig. 7, in addition to $(Ti_{0.8125}W_{0.1875})C_{1.0}$, an attempt was made to determine if there is any tendency for W atoms to segregate in the unit cell before WC phase separation occurs from (Ti,W)C. However, this approach (using a 64-atom unit cell) was unable to discern any tendency for W before phase separation.

Nevertheless, it was possible to explain the formation of a separate WC phase using the formation energy. The formation energy was defined as

$$E_{form} = E_{Ti_xW_{(1-x)}C} - xE_{WC(hcp)} - (1-x)E_{TiC},$$

where $E_{WC(hcp)}$ and E_{TiC} are the total energies of the 64-atom unit cell of WC(*hcp*) and TiC($B1$), respectively. Fig. 10 shows the calculated formation energy of the 64-atom unit cell with the NaCl structures for various W contents. It should be noted that the formation energy is negative when $x < \sim 0.26$, which suggests that $(Ti_{1-x}W_x)C$ with the $B1$ structure is stable. A comparison with the results from ThermoCalc® software ($x < \sim 0.552$) showed that the solubility limit of W in (Ti,W)C increases with decreasing carbon content, thereby losing stoichiometry. This is related to the instability of the NaCl-type WC in stoichiometric $(Ti_{1-x}W_x)C$.

In this study the carbon loss (or presence of vacancies), the size of the W atom, and the instability of WC in a $B1$ structure

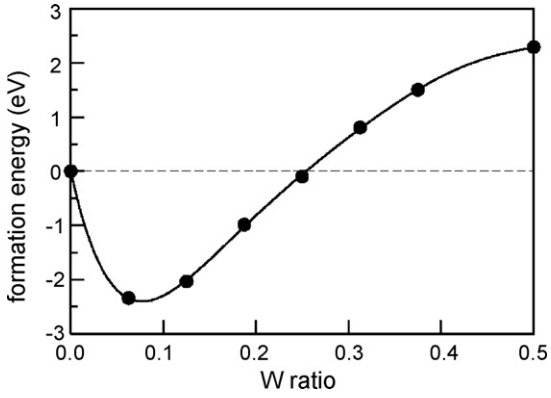

Fig. 10. Calculated formation energy versus W content. The formation energy is negative for $x < \sim 0.26$, which indicates that the $(Ti_{1-x}W_x)C$ alloy with a NaCl structure is stable in that composition range. The solid line is a polynomial fit to the calculated formation energy.

were found to determine the lattice parameters. In particular, the carbon content significantly affects the lattice parameter. The effects of both the carbon loss and the smaller size of the W on the lattice parameters seem to be compensated by the effect of the weak bonding between the W and C in the NaCl($B1$) structure. Furthermore, it is realized that the results of the *ab initio* simulation are in good agreement with the experimental results for high W contents ($x > 0.2$), even without reflecting the nonstoichiometry of this system. The deviation for low W contents is yet to be explained.

4. Summary and conclusions

(Ti,W)C solid solution powders were synthesized to study the effect of W content on the carbon nonstoichiometry and subsequently the lattice parameter. The mechanism of formation of $(Ti_{1-x}W_x)C$ was discussed using simple modeling based on lattice parameters. Furthermore, the behaviors of carbon and

tungsten in $(Ti_{1-x}W_x)C$ were investigated using *ab initio* simulations using a pseudo-potential program. A summary of the conclusions reached in this study is as follows:

(1) The loss of carbon was observed with increasing W in the $(Ti_{1-x}W_x)C_{1-y}$ ceramics. However, the measured carbon content in the sintered ceramics was less sensitive to the change in the W content than predicted by ThermoCalc®.
(2) The lattice parameter of monolithic $(Ti_{1-x}W_x)C_{1-y}$ decreased with increasing W content in the solid solution. This is due to the small atomic radius of W and the loss of carbon for system stability. The changes in the lattice parameter of $(Ti_{1-x}W_x)C_{1-y}$ and the solubility limits of W and C in (Ti,W)C were largely attributed to the instability of WC in the *B*1(*NaCl*) structure.
(3) *Ab initio* simulations with stoichiometric $(Ti_{1-x}W_x)C_{1.0}$ showed that the calculated equilibrium volumes almost obey Vegard's law when W atoms are located randomly at Ti sites. The results match the experimental values for $(Ti_{1-x}W_x)C_{1-y}$. This might be due to the compensating effects of carbon loss and the relatively weak bonding forces between the W and C in the *B*1 structure. This approach (using a 64-atom unit cell) is unsuitable for predicting W separation in a (Ti,W)C system.

Acknowledgements

S. Park, J. Jung and S. Kang acknowledge the research fund from the MOCIE (Ministry of Commerce, Industry and Energy) through a National R&D Project for Nano Science and Technology under contract # M10212430001-02B1543-00210. They also acknowledge grant-in-aid from the National Core Research Center Program from MOST and KOSEF (No. R15-2006-022-R15-2006-022-03001-0). B.W. Jeong, C.-K. Lee and J. Ihm acknowledge the support of the SRC program (Center for Nanotubes and Nanostructured Composites) of MOST/KOSEF, and the Korean Government MOEHRD, Basic Research Fund No. KRF-2006-341-C000015.

References

1. Gee MG, Reece MJ, Roebuck B. High resolution electron microscopy of Ti(C,N) cermets. *J Hard Mater* 1992;**3**(2):119–43.
2. Otsuka T. *Nippon Shinkinzoku KK*; 1983. JP58-213619.
3. Park S, Kang S. Toughened ultra-fine (Ti,W)(CN)-Ni cermets. *Scripta Mater* 2005;**52**(2):129–33.
4. Park S, Kang YJ, Kwon HJ, Kang S. Synthesis of (Ti, M_1, M_2)(CN)–Ni nanocrystalline powders. *Int Ref Metals Hard Mater* 2006;**24**(1–2):115–21.
5. Kim YK, Shim JH, Yang HS, Park JK. Mechanical synthesis of nanocomposite powder for ultrafine (Ti,Mo)C–Ni cermet without core–rim structure. *Int Ref Metals Hard Mater* 2004;**22**(4–5):193–6.
6. Jung, J., A study of the formation and thermo-properties of (Ti,W)(C,N). PhD Thesis, Dept. of Mat. Sci. Eng., Seoul National Univ., 2006.
7. Petersso A, Jansson B, Qvick J, Zackrisson J. M_6C formation during sintering of cemented carbides containing (Ti,W)C. *Int J Ref Met Hard Mater* 2004;**22**(1):21–6.
8. Jhi SH, Ihm J. Electronic structure and structural stability of TiC_xN_{1-x} alloys. *Phys Rev B* 1997;**56**(21):13826–9.
9. Nelson JB, Riley DP. An experimental investigation of extrapolation methods in the derivation of accurate unit-cell. *Proc Phys Soc* 1945;**57**:160–77.
10. Cullity BD. *Element of X-ray Diffraction*. 2nd ed. Addison-Wesley Publishing Company; 1978. p. 102.
11. Ihm J, Zunger A, Cohen ML. Momentum-space formation for the total energy of solids. *J Phys C* 1979;**12**:4409–22.
12. Perdew JP, Wang Y. Accurate and simple density functional for the electronic exchange energy: generalized gradient approximation. *Phys Rev B* 1986;**33**:8800–2.
13. Vanderbilt D. Optimally smooth norm-conserving pseudopotentials. *Phys Rev B* 1985;**32**:8412–5.
14. Vitryanyuk VK, Chaplygin FI, Kostenetskaya GD. Properties of complex TiC–WC carbides in their homogeneity region. I. Preparation and phase and structural analyses of TiC–WC alloys. *Sov Powder Met Metal Ceram* 1971;**10**:547–52.
15. Powder diffraction file, Joint Committee on Powder Diffraction Standards, 1974.
16. Liu AY, Cohen ML. Theoretical study of the stability of cubic WC. *Solid State Commun* 1988;**67**(10):907–10.
17. Häglund J, Guillermet AF, Grimvall G, Körling M. Theory of bonding in transition-metal carbides and nitrides. *Phys Rev B* 1993;**48**(16):11685–91.
18. Rudy, E., Harmon, D.P. and Brukl, C.E., Air Force Doc. Rept., AAFML-TR-65-2, Prt I, vol. **II**, 1965.
19. Storms EK. *The Refractory Carbides*. New York and London: Academic Press Inc.; 1967.
20. Norton JT, Lewis RK. *Adv Met Res Corp* 1963. N63-18389.
21. Upadhyaya GS. *Nature and Properties of Refractory Carbides*. Commack, NY: Nova Science Publication, Inc.; 1996.
22. Price DL, Cooper BR. Total energies and bonding for crystallographic structures in titanium–carbon and tungsten–carbon systems. *Phys Rev B* 1989;**39**:4945–57.
23. Birch F. Elasticity and constitution of the earth interior. *J Geophys Res* 1952;**57**(2):227–86.
24. Vegard L. Die Konstitution der Mischkristalle und die Raumfüllung der Atome. *Z Phys* 1921;**5**:17–26.
25. Lu ZW, Wei SH, Zunger A. First-principles statistical mechanics of structural stability of intermetallic compounds. *Phys Rev B* 1991;**44**:512–44.